

ORIGINAL ARTICLE

Conserved pharmacological rescue of hereditary spastic paraplegia-related phenotypes across model organisms

Carl Julien^{1,†}, Alexandra Lissouba^{1,†}, Surya Madabattula^{3,4,†}, Yasmin Fardghassemi², Cory Rosenfelt⁴, Alaura Androschuk⁴, Joel Strautman^{3,4}, Clement Wong⁴, Andrew Bysice⁴, Julia O'sullivan⁴, Guy A. Rouleau⁵, Pierre Drapeau¹, J. Alex Parker¹ and François V. Bolduc^{3,4,*}

¹CRCHUM and Department of Neuroscience and ²CRCHUM and Department of Biochemistry, Université de Montréal, Montréal, Québec, Canada, ³Institute for Neuroscience and Mental Health and ⁴Department of Pediatrics, University of Alberta, Edmonton, Alberta, Canada and ⁵Montreal Neurological Institute and Hospital, McGill University, Montréal, Québec, Canada

*To whom correspondence should be addressed at: University of Alberta, 3020 Katz Group Centre, 11315 87th Avenue, Edmonton, Alberta, Canada T6G 2E1. Tel: +1 7804929616; Fax: +1 7804920723; Email: fbolduc@ualberta.ca

Abstract

Hereditary spastic paraplegias (HSPs) are a group of neurodegenerative diseases causing progressive gait dysfunction. Over 50 genes have now been associated with HSP. Despite the recent explosion in genetic knowledge, HSP remains without pharmacological treatment. Loss-of-function mutation of the SPAST gene, also known as SPG4, is the most common cause of HSP in patients. SPAST is conserved across animal species and regulates microtubule dynamics. Recent studies have shown that it also modulates endoplasmic reticulum (ER) stress. Here, utilizing null SPAST homologues in *C. elegans*, *Drosophila* and zebrafish, we tested FDA-approved compounds known to modulate ER stress in order to ameliorate locomotor phenotypes associated with HSP. We found that locomotor defects found in all of our spastin models could be partially rescued by phenazine, methylene blue, *N*-acetyl-cysteine, guanabenz and salubrinal. In addition, we show that established biomarkers of ER stress levels correlated with improved locomotor activity upon treatment across model organisms. Our results provide insights into biomarkers and novel therapeutic avenues for HSP.

Introduction

Hereditary spastic paraplegia (HSP) represents a group of neurodegenerative disorders leading to progressive deterioration in gait first described by Strumpel in 1880 (1). Neuropathological changes are most commonly observed in the longest ascending and descending axons of the cortico-spinal tract and ascending axons of the dorsal column neurons (2). HSP can manifest clinically with various patterns. In some patients, motor symptoms and signs are the only manifestations of the disease (known as pure form),

whereas other patients present associated signs of cognitive defects, seizures or sensory symptoms (known as complicated form) (3). Over 50 genes are now associated with HSP (4). Nonetheless, many patients remain without a genetic diagnosis, suggesting that even more genes or unknown causes are involved with HSP. Several cellular pathways are disrupted in HSP. Changes in microtubule dynamics, axonal transport and mitochondrial function are thought to explain the distal end neurodegeneration seen in HSP and could be a common pathological mechanism for several causative genes (5,6).

[†]The first three authors are co-first authors.

Received: May 4, 2015. Revised: November 13, 2015. Accepted: December 29, 2015

© The Author 2016. Published by Oxford University Press. All rights reserved. For Permissions, please email: journals.permissions@oup.com

Mutations in the gene *SPASTIN* represent the most common cause of autosomal dominant (AD) HSP (40% of pure AD-HSP). Most mutations described to date (missense, truncating (5) or splice site mutations (7,8)) lead to loss-of-function via defects in the ATPase Associated with the diverse cellular Activities (AAA) domain (9). So far, most cellular studies have focused on the role of SPAST in microtubule stability and severing from the AAA domain (10,11). Moreover, microtubule modifying drugs such as taxol, vinblastine, epothilone D and noscapine were identified as rescuing peroxisome trafficking deficit in HSPs patient-derived stem cells (12). Previous research of the SPAST homologue in *C. elegans* has identified a microtubule binding region with ATPase microtubule severing activity (13–15). However, little is known about the consequences of mutations in SPAST homologue on locomotion, as much of the previous research has focused on imaging. Loss of function in the *Drosophila* spastin homologue results in microtubule network abnormalities, increased levels of the stabilized acetylated form of microtubules, leads to abnormal axonal arborization and axonal regeneration, and induces, locomotor defects, and early mortality (16–18). Work in zebrafish also revealed that depletion of its SPAST homologue alters microtubules (19), axon outgrowth (20,21), and provokes abnormal endosomal tubulation (22).

Here, we investigated a novel mechanism that could lead to neurodegeneration in HSP, the ER stress response. In addition to its role in microtubule regulation, spastin has also been linked to the endoplasmic reticulum (ER) network (23–26). We have previously shown that methylene blue, salubrinal, guanabenz and phenazine target the ER stress response and protect against proteotoxicity in simple models of another neurodegenerative disorder, amyotrophic lateral sclerosis (27,28). Here, we utilized multiple animal models for spastin including worm, fly and zebrafish in order to investigate if these drugs are able to rescue locomotor and cellular defects observed in SPAST mutant animals. We show that our models of *spastin* loss-of-function present defects in locomotion that can be partially rescued using these compounds. Moreover, improved locomotion correlated with return to wild-type level for biomarkers of ER stress.

Results

MODEL 1: *C. elegans*

spas-1 mutants develop an HSP-related motor phenotype in *C. elegans*

In *C. elegans*, we first examined for HSP-related phenotypes in mutants for the homologous genes SPG1 (L1CAM/*lad-2*), SPG4 (SPAST/*spas-1*) and SPG3A (ATL1/*atln-1*) (Table 1). Interestingly, using paralysis assays, we observed that the *spas-1(ok1608)* ($P < 0.0001$, $N = 83$ –371) and the *spas-1(tm683)* mutants displayed progressive motor defects compared with wild-type N2 worms ($P = 0.0002$, $N = 51$ –371) (Fig. 1A). RT-PCR revealed that *spas-1(ok1608)* mutants display a loss of *spas-1* expression (Fig. 1B). We also observed that the *lad-2(hd-31)* ($P < 0.0001$, $N = 359$ –371) and the *lad-2(tm3056)* ($P < 0.0001$, $N = 234$ –371), but not the

atln-1-related mutant Y54G2A.2(*ok1144*) ($P = 0.4665$, $N = 80$ –371) nematodes exhibit a progressive paralysis phenotype compared with wild-type N2 worms (Supplementary Material, Fig. S1). This is the first time a locomotor defect is shown in *C. elegans* *spastin* mutants.

Guanabenz, salubrinal, phenazine, and methylene blue rescue the motor phenotype in *C. elegans* models of HSPs

We previously identified that methylene blue, salubrinal, guanabenz and phenazine target the ER stress response and have beneficial effects against human mutant TDP-43 neuronal toxicity *in vivo* (27,28). In this study, we first tested these compounds at doses previously found to be efficient (27,28) in our HSP models in *C. elegans* and found that all these drugs rescued the paralysis phenotype of *spas-1(ok1608)* ($P < 0.0001$ –0.0032, $N = 50$ –85) (Fig. 2) and *lad-2(hd31)* mutants ($P < 0.0001$, $N = 64$ –83) (Supplementary Material, Fig. S2).

Guanabenz, salubrinal and methylene blue but not phenazine prolong the lifespan in *spas-1* mutants in *C. elegans*

We next asked whether drugs that beneficially affect the motor phenotype in *spas-1* and *lad-2* mutants could also ameliorate another key marker of these HSP models, their lifespan. We observed that guanabenz, salubrinal and methylene blue, but not phenazine, prolonged the lifespan of *spas-1(ok1608)* ($P < 0.0001$, $N = 65$ –84) (Fig. 3) and *lad-2(hd31)* worms ($P < 0.0001$ –0.0281, $N = 46$ –84) (Supplementary Material, Fig. S3).

Methylene blue, guanabenz, salubrinal and phenazine prevent oxidative stress induced by a *spas-1* mutation in *C. elegans*

In order to identify mechanisms of our compounds on HSP-related motor phenotypes, we first investigated their antioxidant properties, since guanabenz was shown to inactivate nitric oxide synthase (29), salubrinal is known to be a specific inhibitor of the eIF2 α phosphatase enzymes (30) and methylene blue is a monoamine oxidase A inhibitor (31). In addition, phenazine has a structure similar to that of methylene blue. We observed that 10 mM *N*-Acetyl-L-cysteine, a strong antioxidant, reduced the paralysis phenotype in the *spas-1(ok1608)* (Fig. 4A) ($P = 0.0275$, $N = 189$ –199) and in the *lad-2(hd31)* (Supplementary Material, Fig. S4) ($P < 0.0001$, $N = 90$) nematodes. In addition, following 2',7'-dichlorofluorescein diacetate (DCF-DA) exposure, fluorescence measurements at 488 nm revealed that the *spas-1(ok1608)* worms display increased levels of reactive oxygen species (ROS) (Fig. 4B and C) ($P = 0.0067$, $N = 17$ –26). The esterified substrate is cleaved by an esterase activated by ER stress, releasing fluorescein as a marker.

We next wanted to examine if methylene blue, guanabenz, salubrinal and phenazine could have an effect on the oxidative stress detected in the *spas-1* mutants and we observed that all the four compounds reduced the levels of ROS using DCF-DA in the *spas-1(ok1608)* nematodes (Fig. 4B and C) ($P = < 0.0001$ –0.0172, $N = 17$ –26). Thus, these results suggest that the beneficial

Table 1. Human and orthologous genes associated with hereditary spastic paraplegias used in this study

Human gene (protein)	<i>C. elegans</i> orthologous gene	Strain in <i>C. elegans</i> used in this study	<i>Drosophila</i> orthologous gene	Zebrafish orthologous gene
SPG1 - L1CAM (L1 cell adhesion molecule)	<i>lad-2</i>	<i>lad-2(hd31)</i> and <i>lad-2(tm3056)</i>	<i>nrg</i>	<i>nadl1.1</i>
SPG4 - SPAST (Spastin)	<i>spas-1</i>	<i>spas-1(tm683)</i> and <i>spas-1(ok1608)</i>	<i>spas</i>	<i>spast</i>
SPG3A - ATL1 (Atlantastin-1)	<i>atln-1</i>	Y54G2A.2(<i>ok1144</i>)	<i>atl</i>	<i>atl1</i>

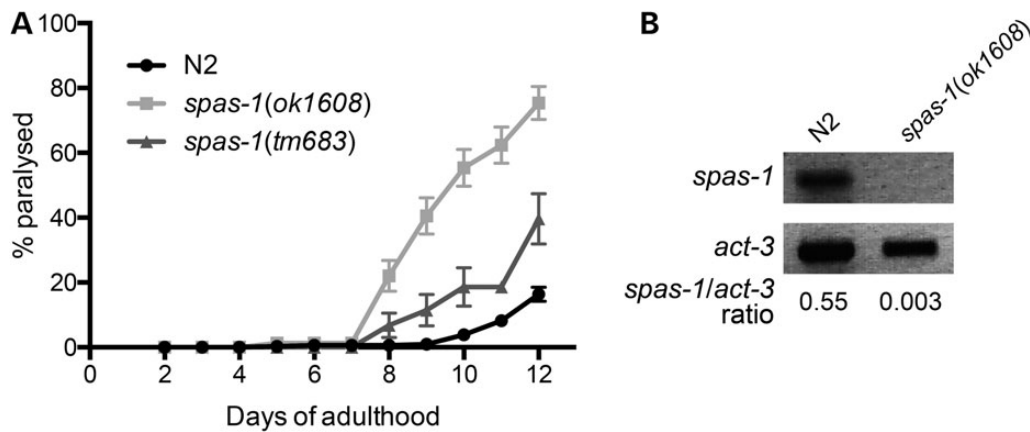


Figure 1. *spas-1* mutation caused age-dependent HSP-related motor phenotype in *C. elegans*. (A) Wild-type N2 nematodes showed no clear paralysis phenotype until the age of Day 12 of adulthood. *spas-1(ok1608)* and *spas-1(tm683)* strains displayed a progressive paralysis phenotype. (B) RT-PCR analysis revealed a loss of expression of the *spas-1* gene in the *spas-1(ok1608)* nematodes.

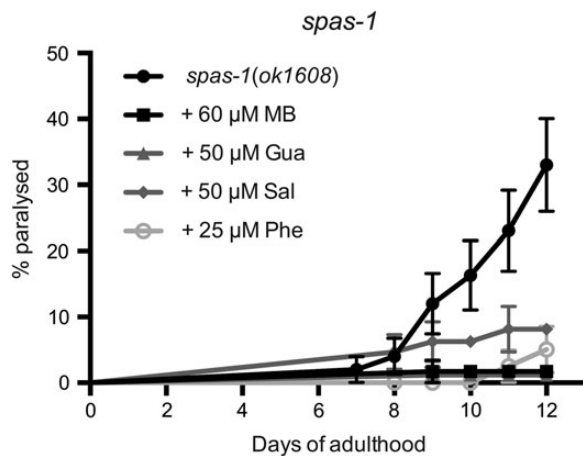


Figure 2. Methylene blue, guanabenz, salubrinal and phenazine prevented the HSP-related motor phenotype in *spas-1* mutation in *C. elegans*. 60 μ M methylene blue (MB), 50 μ M guanabenz (Gua), 50 μ M salubrinal (Sal) and 25 μ M phenazine (Phe) reduced the % of paralysis in *spas-1(ok1608)* worms.

effects of the compounds could be due, at least in part, to their antioxidant properties.

Methylene blue, guanabenz, salubrinal, and phenazine rescue the ER stress response caused by *spas-1* knockdown in *C. elegans*

We previously showed that methylene blue, guanabenz, salubrinal and phenazine increase expression of *hsp-4*, the *C. elegans* ortholog of the protective Hsp70/BiP, which is induced by ER stress (32), using the *zcls4[hsp-4::GFP]* reporter strain (28). Here, we also observed that methylene blue and phenazine induced the expression of *hsp-4*/BiP in the *hsp-4::GFP* reporter strain (Fig. 4D and E) ($P < 0.0003$ – 0.0134 , $N = 23$ – 25). However, we did not observe an increase in *hsp-4*/BiP expression following treatment with guanabenz or salubrinal (Fig. 4D and E). These discrepancies could be due by the treatment parameters. Here, the nematodes were exposed to the compounds from birth to adult day 1, compared with L4 to adult day 1 in the previous study. Also, in this study, the control worms were in a RNA interference (RNAi) experiment paradigm with exposition to an empty vehicle control for RNAi with 1 mM isopropyl- β -D-thiogalactopyranoside (IPTG) compared with only OP50 in the previous study. However, more interestingly here, treatment with the four compounds tested, methylene blue,

guanabenz, salubrinal and phenazine, restored the control *hsp-4*/BiP levels in *spas-1* knockdown using RNAi in *hsp-4::GFP* worms (Fig. 4D and E) ($P < 0.0001$ – 0.0002 , $N = 23$ – 25).

MODEL 2: *Drosophila*

Methylene blue, phenazine, and N-Acetyl-L-cysteine rescue the negative geotaxis defects caused by *spastin* loss of function in *Drosophila*

Considering the beneficial effect of treatments targeting ER stress in worms, we tested if the compounds could also rescue the locomotor defects previously shown in *Drosophila* with *spastin* loss-of-function (13,16,33). First, considering potential variability between animal models, developmental stages, and drug delivery and absorption, we established a dose–response curve for each drugs in our model (Supplementary Material, Fig. S5). We started by using pan-neuronal (*Elav-GAL4*) expression of transgenic RNAi against *spastin*. We observed a significant defect in locomotion compared with wild-type controls ($P \leq 0.001$, $N = 10$), which was rescued using methylene blue ($P \leq 0.01$, $N = 6$) (Fig. 5A and B), phenazine ($P \leq 0.01$, $N = 10$) (Fig. 6A and B) or N-acetyl-L-cysteine ($P \leq 0.05$, $N = 6$) (Fig. 7A and B). We obtained similar results when using the previously extensively characterized *spastin* deletion mutants (*spastin*^{5-75/spastin}¹⁷⁻⁷). They presented severe climbing defects ($P \leq 0.001$, $N = 10$) that were significantly improved after acute treatment of adult flies using methylene blue ($P \leq 0.001$, $N = 7$) (Fig. 5C and D), phenazine ($P \leq 0.01$, $N = 10$) (Fig. 6C and D) and N-Acetyl-L-cysteine ($P \leq 0.01$, $N = 8$) (Fig. 7C and D). None of the drugs had effect on wild-type control flies ($N = 10$).

We performed immunohistochemistry of the *Drosophila* brain and identified increased level of BiP levels in brain of flies with pan-neuronal expression of the *Spas*RNAi used in the behavioral experiments ($N = 5$, $P = 0.0037$) (Fig. 8A, B and D). Treatment with methylene blue restored BiP levels to the level of wild-type flies ($N = 5$, $P = 0.2787$) (Fig. 8B–D).

MODEL 3: Zebrafish

All four compounds partially rescue the morphological phenotype and reduce microtubule defects of the *spastin* morphant in zebrafish

Next, we validated the *C. elegans* and *Drosophila* findings in a vertebrate model. We knocked down *spastin* in zebrafish embryos by injecting an antisense morpholino (MO) against the first translation initiation site of *spastin* (13,16,17). Morphants injected with *spastin* MO but not with an irrelevant control MO (CoMO) had

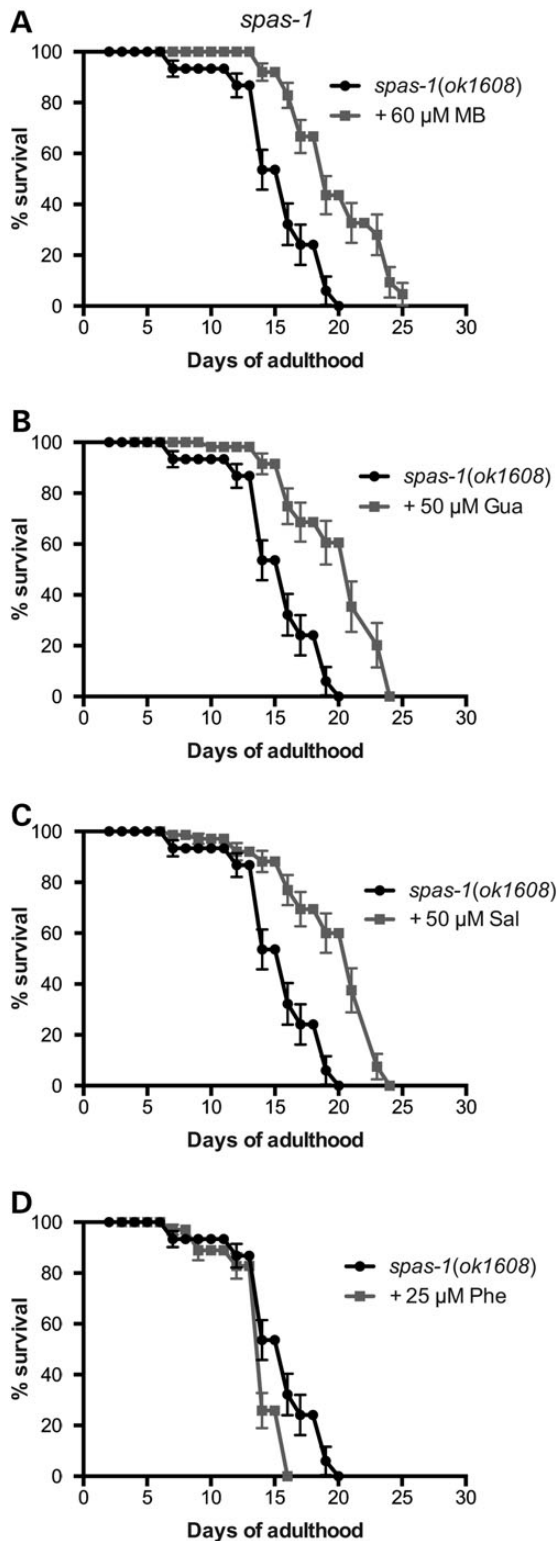


Figure 3. Methylene blue, guanabenz, salubrinal and phenazine extended the lifespan of *spas-1* mutant in *C. elegans*. (A) Methylene blue (MB), (B) guanabenz (Gua) and (C) salubrinal (Sal), (D) but not phenazine (Phe), prolonged the lifespan in *spas-1(ok1608)* mutants in *C. elegans*.

abnormal morphological features, including hydrocephalia, perturbed yolk sac extension and an arched-back phenotype, similar to what has been previously reported with the same MO

(19,20,22), or a splice-blocking MO against exon 7 of *spastin* (19,21). Following a 12-h treatment with either methylene blue, guanabenz, salubrinal or phenazine from 18 hours post fertilization (hpf), these phenotypes were partially rescued, mainly by methylene blue and salubrinal (Fig. 9A and B).

Immunofluorescent staining against acetylated-tubulin showed that *spastin* morphants exhibited disorganized microtubule networks in the spinal cord and thinner microtubules in the spinal motor neuron axons. Similarly, these defects could be partially rescued by a 12-h incubation with either methylene blue, guanabenz, salubrinal or phenazine (Fig. 9C).

We assessed the levels of oxidative stress in the fish using DCF-DA. Similar to what was obtained in the other two models, a strong fluorescent signal was observed upon the knockdown of *spastin*, compared with the use of a CoMO. This fluorescent signal was reduced by treatment with any of the 4 ER-modulating drugs (Fig. 9D and E). Collectively, these data suggest that methylene blue, guanabenz, salubrinal and phenazine are able to reduce the level of oxidative stress generated by the loss-of-function of *spastin*.

Taken together, these results show that methylene blue, salubrinal, and to a lesser extent guanabenz and phenazine can partially rescue the morphological phenotype and microtubule defects in a vertebrate genetic model of HSP.

Discussion

HSP represents a group of neurodegenerative disorders causing progressive gait impairment. HSPs are caused by over 50 genes and remain without pharmacological treatment. Here, we targeted the most common HSP gene, *SPASTIN*, in three model organisms, *C. elegans*, *Drosophila* and the vertebrate zebrafish.

Recent evidence linking HSP to ER stress prompted us to investigate the oxidative stress inhibitors as a potential means to alleviate the phenotypic manifestations of HSP. Previous success of oxidative stress inhibitors with another neurodegenerative disease, amyotrophic lateral sclerosis (ALS), led us to consider the role of the same compounds—phenazine, guanabenz, salubrinal, methylene blue and *N*-acetyl-cysteine as potential therapeutic agents in our HSP models of disease. All selected therapeutic agents, with the exception of phenazine, are FDA approved and could rapidly be translated into clinical trials. We show for the first time that inhibition of ER stress may be key at preventing microtubule disorganization, which is a common feature of many genes involved in HSP. Our data suggest that *spastin* knockdown induces the ER stress response, and that treatments with the compounds examined in this study rescue this exacerbated response. We also found that both lifespan and locomotion were rescued in our three model organisms with *spastin* mutations.

Future work will be required to extend our findings to other mammalian models but using FDA-approved compounds is likely to accelerate the application to clinical trials for HSP patients.

Material and Methods

MODEL 1: *C. elegans* experiments

Strains and genetics

Standard methods of culturing and handling worms were used. Worms were maintained on standard nematode growth media (NGM) plates streaked with OP50 *E. coli*. All strains were scored at 20°C. Mutations used in this study were: *lad-2(hd-31)*, *lad-2(tm3056)*, *spas-1(ok1608)*, *spas-1(tm683)*, Y54G2A.2(*ok1144*). Mutant strains were obtained from the *C. elegans* Genetics Center

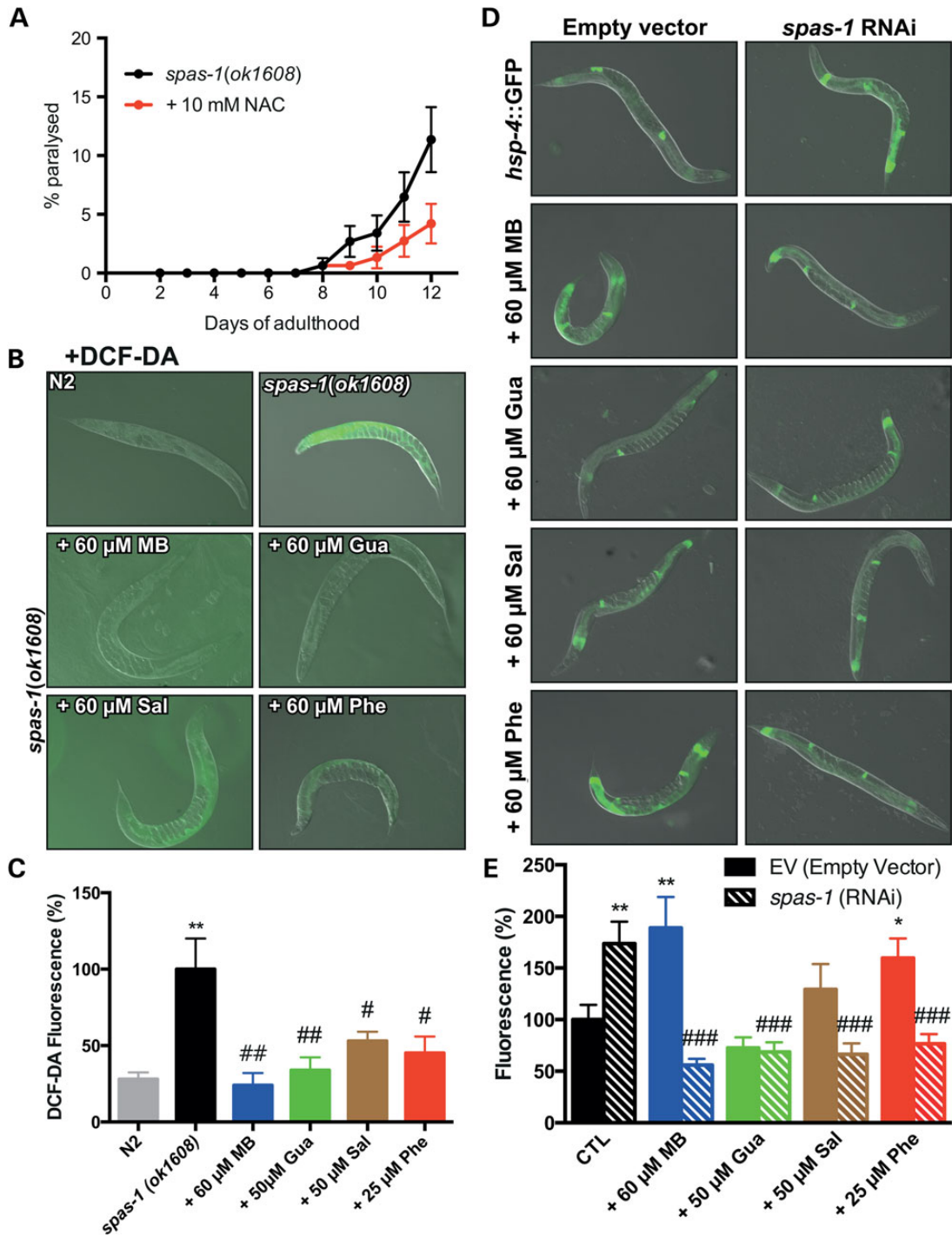


Figure 4. Oxidative stress is associated with the paralysis observed in the *spas-1* mutants, and methylene blue, guanabenz, salubrin and phenazine prevent this oxidative stress in *spas-1* mutant nematodes. (A) 10 mM N-Acetyl-L-cysteine (NAC), a strong antioxidant, reduced the % of paralysis in the *spas-1(ok1608)* nematodes. (B) 2',7'-dichlorofluorescein diacetate (DCF-DA) fluorescent photos and (C) quantification of *spas-1(ok1608)* worms after treatment with methylene blue (MB), guanabenz (Gua), salubrin (Sal) and phenazine (Phe). ** $P < 0.01$ versus N2 controls; * $P < 0.05$, ## $P < 0.01$ versus *spas-1(ok1608)* nematodes (Student's t-tests). Silencing *spas-1* induces the ER-related *hsp-4*/BiP expression, and methylene blue, guanabenz, salubrin and phenazine prevent this *hsp-4* increase in *C. elegans*. (D) Representation and (E) quantification of *spas-1* RNAi which induces the *hsp-4*/BiP expression in the *zcls4[hsp-4::GFP]* worms, but exposure to methylene blue (MB), guanabenz (Gua), salubrin (Sal) and phenazine (Phe) prevent this *hsp-4::GFP* increase. * $P < 0.05$, ** $P < 0.01$ versus untreated empty vector (EV) controls, ### $P < 0.001$ versus untreated *spas-1* RNAi (Student's t-tests).

(University of Minnesota, Minneapolis, MN, USA). Deletion mutant were verified by PCR and each had been outcrossed a minimum of three times to wild-type N2 worms prior to use.

Paralysis assay

Mutant *lad-2*, *spas-1*, Y54G2A.2 were scored for paralysis from adult day 1 to adult day 12 as described previously (34–36). Briefly,

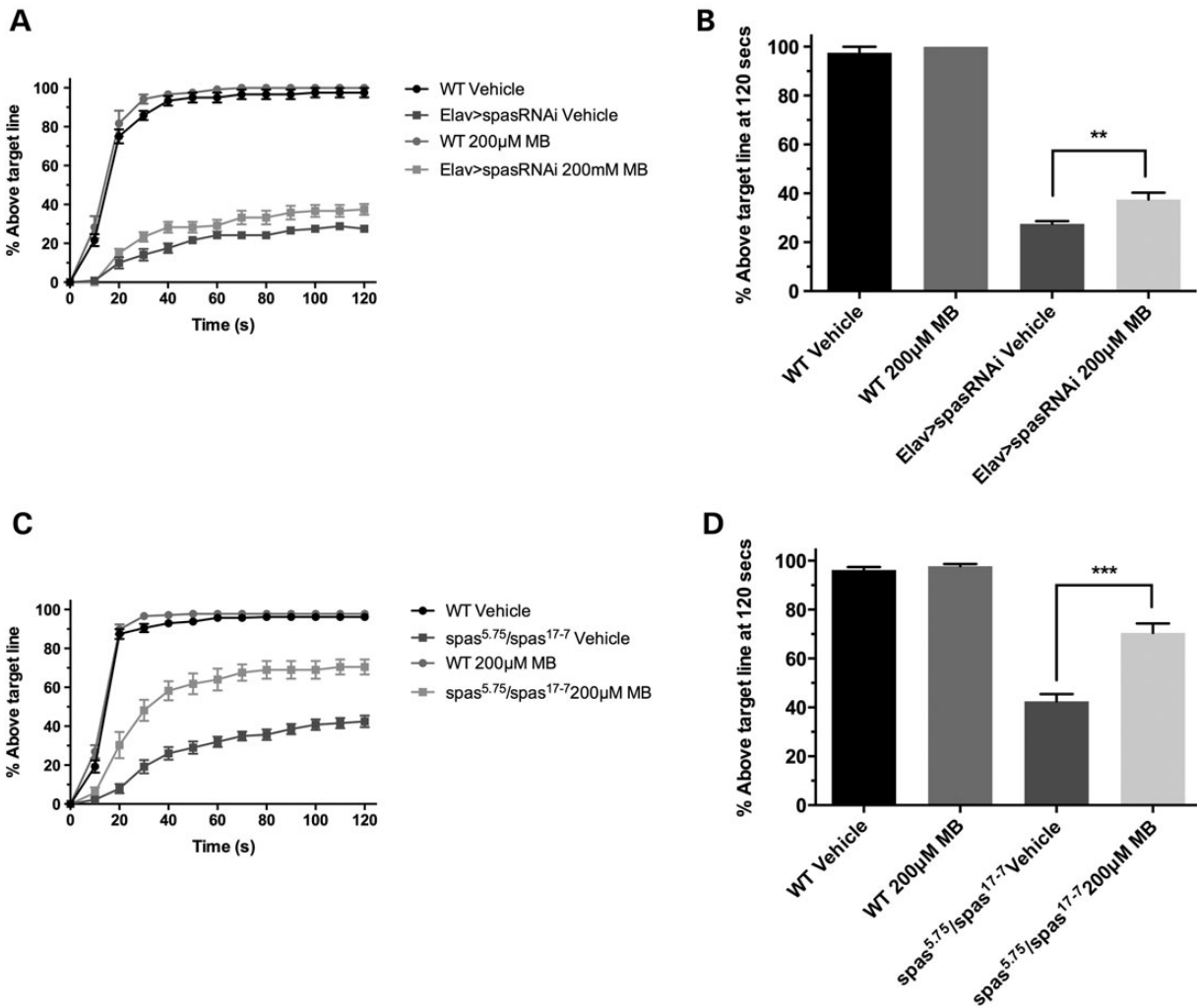


Figure 5. Methylen blue rescues the locomotor defects caused by *spastin* loss-of-function in *Drosophila*. (A) Flies expressing pan-neuronal RNAi against *spastin* display poor climbing performance ($N = 6$) which is rescued with overnight Methylen blue treatment. (B) Significantly increased climbing performance is observed at 2 min with *spastin* RNAi transgenic flies treated with Methylen blue ($P \leq 0.01$, t-test). (C) Transheterozygous *spastin* mutants (*spastin*^{5.75}/*spastin*¹⁷⁻⁷) display poor climbing performance ($N = 7$) which is rescued with overnight Methylen blue treatment. (D) Significantly increased climbing performance is observed at 2 min with transheterozygous flies treated with Methylen blue ($P \leq 0.001$, t-test).

30 L4 animals were transferred to NGM-FUDR and, the subsequent days, were counted as positive if they failed to move after being prodded with a worm pick. Worms scored as dead if they failed to move their head after prodding on the nose.

Lifespan assay

For lifespan assay, thirty L4 *lad-2*, *spas-1*, Y54G2A.2 mutants were transferred on NGM-FUDR plates and tested daily from adult day 1 until death. Worms were scored as dead if they failed to respond to tactile stimulus.

Drug exposure

The nematodes were exposed from birth to 60 µM methylen blue, 50 µM salubrinal, 50 µM guanabenz, 25 µM phenazine or 10 mM N-Acetyl-L-cysteine incorporated into NGM solid medium or NGM solid medium only as control. All the medium plates were streaked with OP50 *E. coli*. Compounds were purchased from Sigma-Aldrich (St. Louis, MO, USA) and Tocris Bioscience (Ellisville, MO, USA). Briefly, ~5–7 adult hermaphrodites were placed on solid media with or without the drugs for 3–4 days

and kept at 20°C. Then, ~30 L4 worms were picked were plated on corresponding NGM-FUDR medium and behavioral tests, life-span assays and fluorescence microscopy were performed.

RT-PCR assays

RNA samples were obtained from 15 confluent plates of worms, following Trizol (Invitrogen)/chloroform extraction and quantified with a Nano-Photometer (Implen). One microgram of RNA were reverse transcribed preceded by gDNA wipeout. One microliter of cDNA was used for *spas-1* amplification using the following primers: forward, 5'-TGAGAGCCCGATTGAAATGG-3'; C24B5.2 reverse, 5'-TCTGATTCACCTTCTCCGGGTTT-3'.

Reactive oxygen species measurements

The *in vivo* detection of ROS in *C. elegans* is previously described (27,28). Briefly, worms were incubated on a slide with 5 µM 2',7'-dichlorofluorescein diacetate (DCF-DA, Sigma-Aldrich) for 30 min at room temperature and washed three times for 5 min with PBS 1X. N2 wild type and *spas-1(ok1608)* mutants worms 2 days aged were visualized by fluorescence microscopy under a

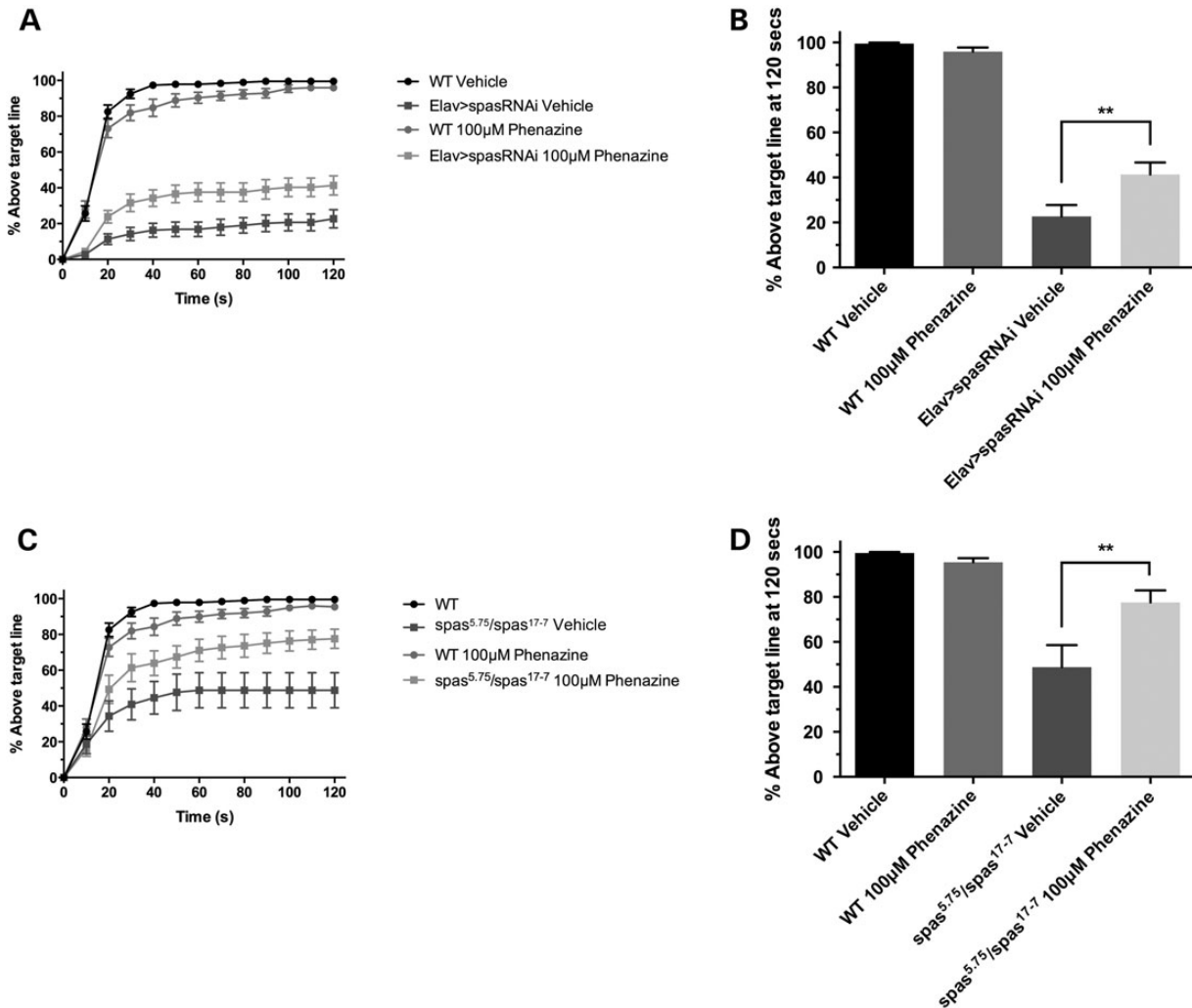


Figure 6. Phenazine rescues the locomotor defects caused by *spastin* loss-of-function in *Drosophila*. (A) Flies expressing pan-neuronal RNAi against *spastin* display poor climbing performance ($N = 10$) which is rescued with overnight phenazine treatment. (B) Significantly increased climbing performance is observed at 2 min with *spastin* RNAi transgenic flies treated with phenazine ($P \leq 0.01$, t-test). (C) Transheterozygous *spastin* loss-of-function mutants (*spastin*^{5.75}/*spastin*^{17.7}) display poor climbing performance ($N = 10$) which is rescued with overnight phenazine treatment. (D) Significantly increased climbing performance is observed at 2 min with transheterozygous flies treated with methylene blue ($P \leq 0.01$, t-test).

488 nm wavelength excitation. The ROS was expressed as percentage of *spas-1(ok1608)* mutants.

RNAi experiments

RNAi-treated *hsp-4::GFP* worms were fed *E. coli* (HT115) containing an empty vector or *E. coli* expressing dsRNA against *spas-1* (C24B5.2). The RNAi clone was from the ORFeome RNAi library (Open Biosystems). RNAi experiments were performed at 20°C. Worms were grown on NGM enriched with 1 mM isopropyl- β -D-thiogalactopyranoside. Synchronized L1 worms were grown on plates with RNAi bacteria until adult day 1, when they were assayed for fluorescence microscopy.

Fluorescence microscopy

For visualization of *hsp-4::GFP* and DCF-DA-exposed animals, M9 buffer with 60% glycerol was used for immobilization. Animals were mounted on slides with 2% agarose pads and examined for fluorescence. Fluorescent expression for quantification was visualized with a Zeiss Axio Imager M2 microscope. Fluorescent expression was visualized with a DIC microscope Carl Zeiss AxioObserver A1. The software used was AxioVs40 4.8.2.0.

Twenty-seven to thirty-three worms were visualized. Image processing and quantification were done with Adobe Photoshop. To compare fluorescence, we calculated the changes in the ratio (size/intensity of fluorescence).

Statistics

Paralysis and lifespan curves were generated and compared using the Log-rank (Mantel-Cox) test. All experiments were repeated at least three times. For fluorescence, parametric Student's t-tests were realized. Prism 6 (GraphPad Software) was used for all statistical analyses.

MODEL 2: *Drosophila* experiments

Fly stocks

Drosophila were raised at 22°C with 40% humidity. *Drosophila spastin*^{5.75/Tb} and *spastin*^{17.7}/TAGS were a generous gift of Dr Nina Sherwood (Duke University). *Drosophila spastin* RNAi transgenic were obtained from the Vienna *Drosophila* RNAi center. The transgenic line used for this study is # U108739. Flies were raised in incubator with a 12:12 light:dark cycle.

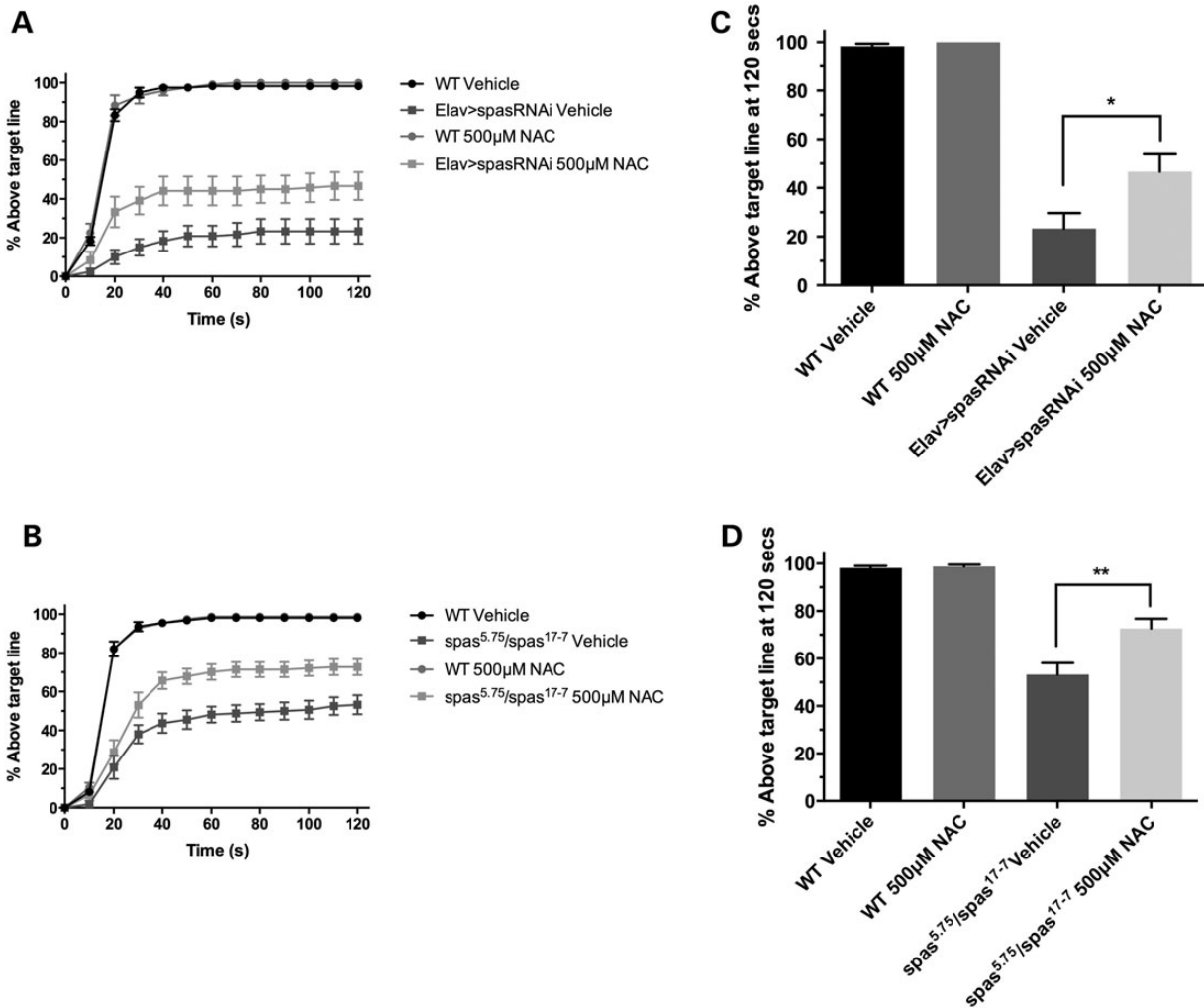


Figure 7. *N*-Acetyl-L-cysteine rescues the locomotor defects caused by *spastin* loss-of-function in *Drosophila*. (A) Flies expressing pan-neuronal RNAi against *spastin* display poor climbing performance ($N = 6$) which is rescued with overnight *N*-Acetyl-L-cysteine treatment. (B) Significantly increased climbing performance is observed at 2 min with *spastin* RNAi transgenic flies treated with *N*-Acetyl-L-cysteine ($P \leq 0.05$, *t*-test). (C) Transheterozygous *spastin* mutants (*spastin*⁵⁻⁷⁵/*spastin*¹⁷⁻⁷) display poor climbing performance ($N = 8$) which is rescued with overnight *N*-Acetyl-L-cysteine treatment. (D) Significantly increased climbing performance is observed at 2 min with transheterozygous flies treated with *N*-Acetyl-L-cysteine ($P \leq 0.01$, *t*-test).

Negative geotaxis (Climbing) assay

Climbing testing was performed as described previously (33). Briefly, 20 flies (1 day old) are collected the day before the experiments in food vials containing either the vehicle or the drug being studied. Flies are transferred into a 250 ml glass cylinder and displaced to the bottom of the cylinder by tapping against soft rubber padding. The number of flies above the target distance of 17.5 cm is recorded over a total time of 2 min. The percentage of flies above the target line versus the total number of flies is represented at every 10-s intervals.

Statistical analysis comparing the performance of flies in the vehicle group (fed fly media plus vehicle) versus the drug group (containing both fly media and drug) is performed with a *t*-test (GraphPad Prism). All graphs depict mean \pm SEM.

Pharmacological treatment

Drosophila were raised on standard food media and transferred to vials containing drug dissolved in food. Flies were collected and placed on the drug or regular food around noon the day before testing. Testing occurred the following day from 9 to 12 h.

Drugs used for these experiments include phenazine (Sigma P13207), methylene blue (Sigma M9140) and *N*-Acetyl-cysteine (Sigma A7250). For phenazine, doses tested ranged from 75 to 150 μ m. For methylene blue, doses tested ranged from 50 to 300 μ m. For *N*-Acetyl-cysteine, dose tested ranged from 100 to 750 μ m. Methylene blue and NAC were dissolved in water to make concentrated stock solutions. Phenazine was solubilized in pure DMSO to form a concentrated stock solution. The required amount of stock solution was dissolved in standard food. Drug was added to food when cooled at 60°C.

Immunohistochemistry

One to three days old female flies were dissected and processed as previously described (37). Flies were selected if the food colorant used in the drug treatment was seen in the abdomen to control for drug intake. Flies were dissected in 1X PBS and the brains were transferred to 4% paraformaldehyde (PFA) to fix for 10 min at room temperature. Following the 10-min fixation period, the brains were placed in a vacuum for 1.5 h in a solution of 0.25% Triton 4% PFA. The brains were then incubated in a penetration/

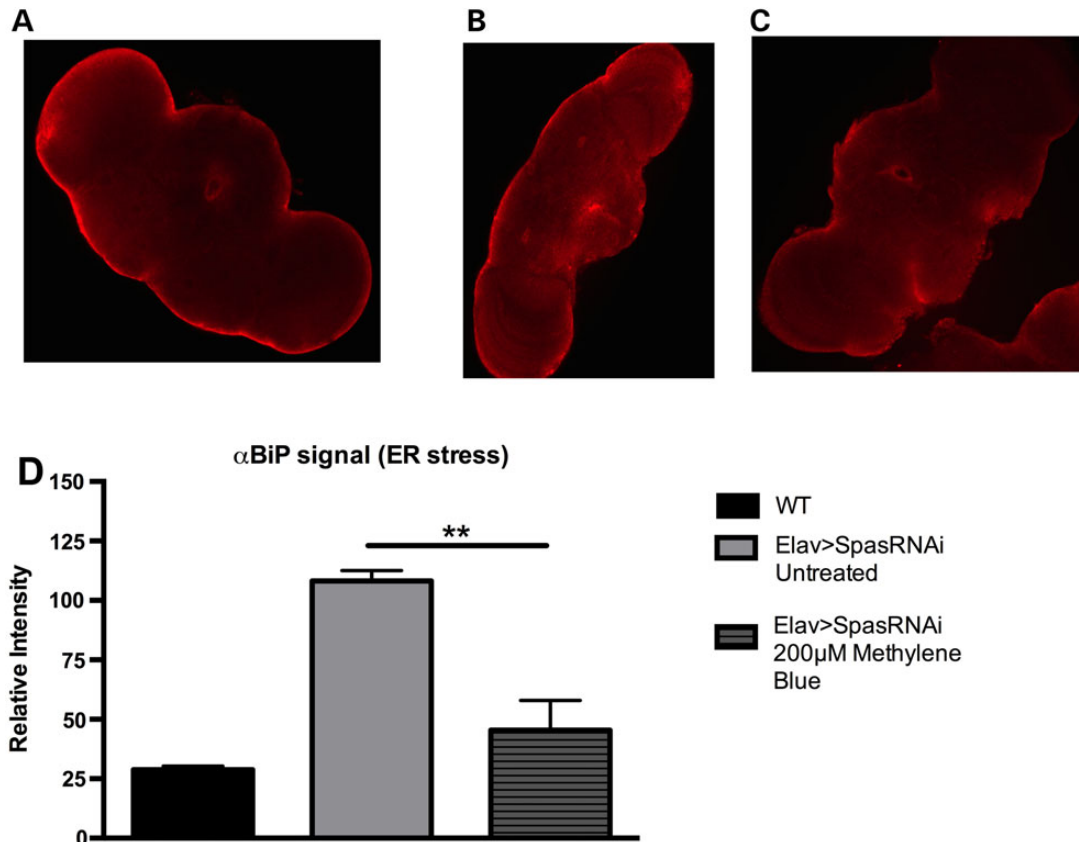


Figure 8. Methylene blue rescues exaggerated oxidative stress caused by *spastin* loss-of-function in *Drosophila*. Representative confocal images of BiP immunostaining in (A) wild-type, (B) *spastin* RNAi expressing flies treated with vehicle and (C) *spastin* RNAi flies treated with methylene blue. (D) Flies expressing pan-neuronal RNAi against *spastin* display elevated BiP level compared with wild-type flies. This level is rescued to normal level by the administration of methylene blue provided in the negative geotaxis experiments ($N = 5$, $P < 0.01$, t-test).

blocking buffer [2% phosphate buffered saline with Tween (PBST), 10% normal goat serum (NGS), 0.02% Sodium Azide] on rocker for 2 h at 4°C and following completion transferred to primary antibody solution (1:50 α -GRP78/HSPA5 (ThermoFisher Scientific PA5-22967) in 1% PBST with 0.25% NGS) and incubated overnight at 4°C. Following overnight incubation, brains were washed 3 times in 1% PBST for 20 min. Brains were subsequently incubated with secondary antibody solution (1:200 Cy3 α -Rabbit Jackson ImmunoResearch 111-165-003) overnight at 4°C. Following incubation with secondary antibody, brains were washed three times with 1% PBST and mounted. Imaging was completed using Zeiss LSM 700 confocal microscope and images were quantified using ImageJ.

MODEL 3: Zebrafish experiments

Maintenance

Zebrafish (*Danio rerio*) embryos were collected and staged using standard methods (27). The local animal care committee at the CRCHUM, having received the protocol relevant to this project relating to animal care and treatment, certified that the care and treatment of animals was in accordance with the guidelines and principles of the Canadian Council on Animal Care. Further, all matters arising from this proposal that related to animal care and treatment, and all experimental procedures proposed for use with animals were reviewed and approved by the committee before they were initiated or undertaken. This review process was ongoing on a regular basis during the entire period that the

research was being undertaken. Zebrafish embryos (no adults were used) are insentient to pain. Fish embryos were incubated for 12 h in each compound, examined and then disposed. Zebrafish embryos were used over a two-day period then terminated.

MO injections

MO (Spast MO: 5'-ATTCATTACCCCTTCTCGGGCTCTC-3') against *spastin* translation initiation site was obtained from Gene Tools and described earlier (19). As a control, an irrelevant MO was used (CoMO: 5'-CCTCTTTACCTCAGTTACAATTTATA-3'). The MOs were diluted in deionized water with 0.05% Fast Green vital dye (Sigma-Aldrich) and 10 ng per embryo was pulse-injected into 1–2 cell stage embryos using a Picospritzer III pressure ejector.

Drug treatments

Eighteen hpf embryos injected with Spast Mo or CoMO were placed in individual wells in a 24 well plate and were treated for 12 h with methylene blue (60 μ M), salubrinal (20 μ M), guanabenz (20 μ M) or phenazine (20 μ M) diluted in Evans solution (in mM): 134 NaCl, 2.9 KCl, 2.1 CaCl₂, 1.2 MgCl₂, 10 HEPES, 10 glucose, pH 7.8, 290 mOsm, with 0.1% DMSO. The embryos were then morphologically assessed and fixed for immunohistochemistry.

Immunostaining

Monoclonal antibody anti-acetylated tubulin were used to assess the microtubule integrity in the spinal cord and motor neuron

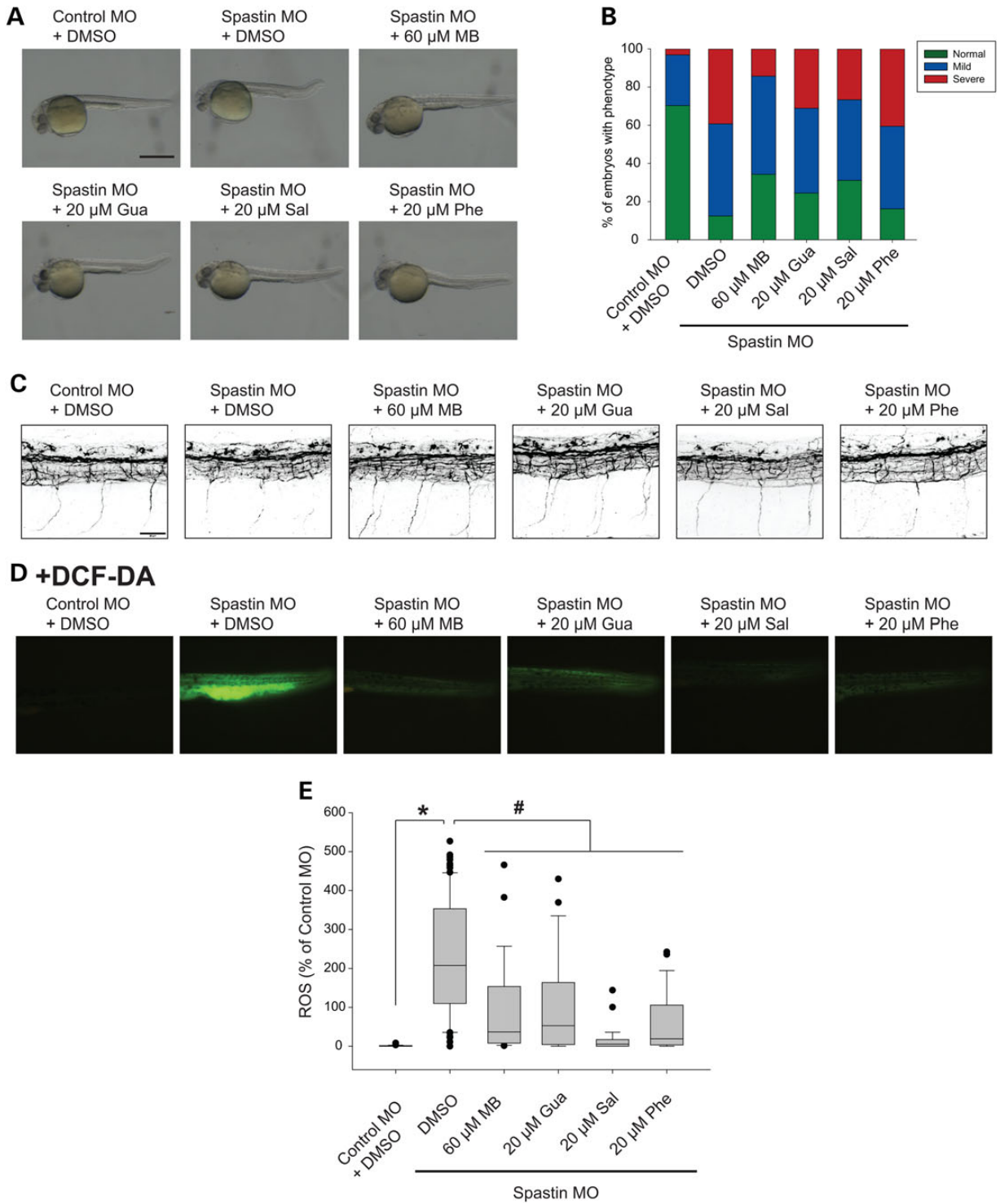


Figure 9. Methylene blue, guanabenz, salubrinal and phenazine partially rescue the morphological phenotype and reduce microtubule defects of the zebrafish *spastin* morphant. (A) Zebrafish embryos at 30 hours post fertilization (hpf). *spastin* morphant embryos show abnormal morphological features compared with embryo injected with control morpholino. Arrows show defects in the head, yolk sac extension and tail. These defects are partially rescued by 60 μM methylene blue (MB), 20 μM guanabenz (Gua), 20 μM salubrinal (Sal) and 20 μM phenazine (Phe). Scale bar is 500 μm. (B) Quantification of morphological defects shown in (A). (C) Whole-mount immunohistochemistry of 30 hpf zebrafish embryos labeled with a microtubule marker. A lateral view of the trunk is shown, with the rostral side of the embryo to the left. *spastin* morphants show a disorganized spinal cord, with thin microtubules at the level of the motor neuron axons. These defects are partially rescued by 60 μM methylene blue (MB), 20 μM guanabenz (Gua), 20 μM salubrinal (Sal) and 20 μM phenazine (Phe). Scale bar is 30 μm, MO: morpholino. (D) Zebrafish embryos injected with a control morpholino show very low level of fluorescence when treated with 2',7'-dichlorofluorescein diacetate (DCF-DA) (a biomarker for oxidative stress) compared with embryos injected with a morpholino against *spastin*. Methylene blue, guanabenz, salubrinal and phenazine reduced the fluorescence. (E) Quantification of fluorescence in DCF-DA-treated embryos show a significant reduction of fluorescence upon treatment with the 4 drugs (* $P < 0.001$ versus control morphant embryos; # $P < 0.01$ versus *spastin* morphant embryos).

axons at 30 hpf. Embryos were fixed with Dent's fixative (80% methanol, 20% DMSO), in order to preserve microtubules, at 4°C overnight. After the fixation, embryos were progressively rehydrated in 75, 50 and 25% methanol in PBS and washed several times in PBST before block. The embryos were incubated overnight at 4°C in primary monoclonal antibody anti-acetylated tubulin (Sigma-Aldrich, 1:500), washed in PBST for a day, then incubated in the secondary antibody conjugated with Alexa Fluor 488 (Molecular Probes, Carlsbad, CA, USA, 1:1000) for 4–6 h at room temperature. Embryos were washed several times in PBS, cleared in 70% glycerol and mounted. Fluorescent images of fixed embryos were taken using a Quorum Technologies spinning-disk confocal microscope mounted on an upright Olympus BX61W1 fluorescence microscope equipped with an Hamamatsu ORCA-ER camera. Image acquisition was performed with Velocity software (PerkinElmer) and images were processed using ImageJ (NIH).

ROS measurements

The *in vivo* detection of ROS was done as before (27,28). Briefly, live 30 hpf were incubated in 5 µm 2',7'-dichlorofluorescein diacetate (DCF-DA) (Sigma-Aldrich) for 20 min at 28.5°C and washed three times for 5 min with embryo media. Fluorescence was observed under a 488 nm wavelength excitation. The ROS was expressed as percentage of control.

Statistical analysis

Significance was determined using two-way ANOVA and Holm-Sidak method of comparison were used for non-normal distributions.

Supplementary Material

Supplementary Material is available at HMG online.

Acknowledgements

We would like to thank Dr N Sherwood for the *Drosophila spastin* mutant flies. We thank VDRC for *Drosophila* RNAi stocks.

Conflict of Interest statement. None declared.

Funding

Some worm strains were provided by the CGC, which is funded by NIH Office of Research Infrastructure Programs (P40 OD010440). This research was funded by the Canadian Institute of Health Research-CIHR (G.A.R., P.D., J.A.P. and F.V.B.). C.J. is supported by CIHR and Huntington's Society of Canada fellowships. A.L. is supported by a CIHR and ALS Canada scholarship. P.D. and G.A.R. hold Canada Research Chairs. J.A.P. holds a career development award from the Fonds de recherche du Québec-Santé. F.V.B. holds a career development award from the Canadian Child Health Clinician Scientist Program (CCHCSP).

References

- McDermott, C., White, K., Bushby, K. and Shaw, P. (2000) Hereditary spastic paraparesis: a review of new developments. *J. Neurol. Neurosurg. Psychiatry*, **69**, 150–160.
- Behan, W.M. and Maia, M. (1974) Strümpell's familial spastic paraplegia: genetics and neuropathology. *J. Neurol. Neurosurg. Psychiatry*, **37**, 8–20.
- Schule, R. and Schols, L. (2011) Genetics of hereditary spastic paraplegias. *Semin. Neurol.*, **31**, 484–493.
- Fink, J.K. (2013) Hereditary spastic paraplegia: clinico-pathologic features and emerging molecular mechanisms. *Acta Neuropathol.*, **126**, 307–328.
- Salinas, S., Proukakis, C., Crosby, A. and Warner, T.T. (2008) Hereditary spastic paraplegia: clinical features and pathogenetic mechanisms. *Lancet Neurol.*, **7**, 1127–1138.
- Hedera, P., DiMauro, S., Bonilla, E., Wald, J.J. and Fink, J.K. (2000) Mitochondrial analysis in autosomal dominant hereditary spastic paraplegia. *Neurology*, **55**, 1591–1592.
- Svenson, I.K., Ashley-Koch, A.E., Pericak-Vance, M.A. and Marchuk, D.A. (2001) A second leaky splice-site mutation in the spastin gene. *Am. J. Hum. Genet.*, **69**, 1407–1409.
- Svenson, I.K., Ashley-Koch, A.E., Gaskell, P.C., Riney, T.J., Cumming, W.J., Kingston, H.M., Hogan, E.L., Boustany, R.M., Vance, J.M., Nance, M.A. et al. (2001) Identification and expression analysis of spastin gene mutations in hereditary spastic paraplegia. *Am. J. Hum. Genet.*, **68**, 1077–1085.
- Salinas, S., Carazo-Salas, R.E., Proukakis, C., Schiavo, G. and Warner, T.T. (2007) Spastin and microtubules: functions in health and disease. *J. Neurosci. Res.*, **85**, 2778–2782.
- Errico, A., Claudiani, P., D'Addio, M. and Rugarli, E.I. (2004) Spastin interacts with the centrosomal protein NA14, and is enriched in the spindle pole, the midbody and the distal axon. *Hum. Mol. Genet.*, **13**, 2121–2132.
- Evans, K.J., Gomes, E.R., Reisenweber, S.M., Gundersen, G.G. and Lauring, B.P. (2005) Linking axonal degeneration to microtubule remodeling by Spastin-mediated microtubule severing. *J. Cell. Biol.*, **168**, 599–606.
- Fan, Y., Wali, G., Sutharsan, R., Bellette, B., Crane, D.I., Sue, C. M. and Mackay-Sim, A. (2014) Low dose tubulin-binding drugs rescue peroxisome trafficking deficit in patient-derived stem cells in Hereditary Spastic Paraplegia. *Biol. Open*, **3**, 494–502.
- Matsushita-Ishiodori, Y., Yamanaka, K., Hashimoto, H., Esaki, M. and Ogura, T. (2009) Conserved aromatic and basic amino acid residues in the pore region of *Caenorhabditis elegans* spastin play critical roles in microtubule severing. *Genes Cells*, **14**, 925–940.
- Matsushita-Ishiodori, Y., Yamanaka, K. and Ogura, T. (2007) The *C. elegans* homologue of the spastic paraplegia protein, spastin, disassembles microtubules. *Biochem. Biophys. Res. Commun.*, **359**, 157–162.
- Yu, W., Qiang, L., Solowska, J.M., Karabay, A., Korulu, S. and Baas, P.W. (2008) The microtubule-severing proteins spastin and katanin participate differently in the formation of axonal branches. *Mol. Biol. Cell*, **19**, 1485–1498.
- Sherwood, N.T., Sun, Q., Xue, M., Zhang, B. and Zinn, K. (2004) *Drosophila* Spastin regulates synaptic microtubule networks and is required for normal motor function. *PLoS Biol.*, **2**, e429.
- Trotta, N., Orso, G., Rossetto, M.G., Daga, A. and Broadie, K. (2004) The hereditary spastic paraplegia gene, spastin, regulates microtubule stability to modulate synaptic structure and function. *Curr. Biol.*, **14**, 1135–1147.
- Stone, M.C., Rao, K., Gheres, K.W., Kim, S., Tao, J., La Rochelle, C., Folker, C.T., Sherwood, N.T. and Rolls, M.M. (2012) Normal spastin gene dosage is specifically required for axon regeneration. *Cell Rep.*, **2**, 1340–1350.
- Wood, J.D., Landers, J.A., Bingley, M., McDermott, C.J., Thomas-McArthur, V., Gleadall, L.J., Shaw, P.J. and Cunliffe, V.T. (2006) The microtubule-severing protein Spastin is essential for axon outgrowth in the zebrafish embryo. *Hum. Mol. Genet.*, **15**, 2763–2771.

20. Butler, R., Wood, J.D., Landers, J.A. and Cunliffe, V.T. (2010) Genetic and chemical modulation of spastin-dependent axon outgrowth in zebrafish embryos indicates a role for impaired microtubule dynamics in hereditary spastic paraplegia. *Dis. Model. Mech.*, **3**, 743–751.
21. Zhang, C., Li, D., Ma, Y., Yan, J., Yang, B., Li, P., Yu, A., Lu, C. and Ma, X. (2012) Role of spastin and protrudin in neurite outgrowth. *J. Cell. Biochem.*, **113**, 2296–2307.
22. Allison, R., Lumb, J.H., Fassier, C., Connell, J.W., Ten Martin, D., Seaman, M.N.J., Hazan, J. and Reid, E. (2013) An ESCRT-spastin interaction promotes fission of recycling tubules from the endosome. *J. Cell Biol.*, **202**, 527–543.
23. Mannan, A.U., Boehm, J., Sauter, S.M., Rauber, A., Byrne, P.C., Neesen, J. and Engel, W. (2006) Spastin, the most commonly mutated protein in hereditary spastic paraplegia interacts with Reticulon 1 an endoplasmic reticulum protein. *Neurogenetics*, **7**, 93–103.
24. Rismanchi, N., Soderblom, C., Stadler, J., Zhu, P.-P. and Blackstone, C. (2008) Atlastin GTPases are required for Golgi apparatus and ER morphogenesis. *Hum. Mol. Genet.*, **17**, 1591–1604.
25. Hu, J., Shibata, Y., Zhu, P.-P., Voss, C., Rismanchi, N., Prinz, W. A., Rapoport, T.A. and Blackstone, C. (2009) A class of dynamin-like GTPases involved in the generation of the tubular ER network. *Cell*, **138**, 549–561.
26. Orso, G., Pendin, D., Liu, S., Tosetto, J., Moss, T.J., Faust, J.E., Micaroni, M., Egorova, A., Martinuzzi, A., McNew, J.A. et al. (2009) Homotypic fusion of ER membranes requires the dynamin-like GTPase atlastin. *Nature*, **460**, 978–983.
27. Vaccaro, A., Patten, S.A., Ciura, S., Maios, C., Therrien, M., Drapeau, P., Kabashi, E. and Parker, J.A. (2012) Methylene blue protects against TDP-43 and FUS neuronal toxicity in *C. elegans* and *D. rerio*. *PLoS One*, **7**, e42117.
28. Vaccaro, A., Patten, S.A., Aggad, D., Julien, C., Maios, C., Kabashi, E., Drapeau, P. and Parker, J.A. (2013) Pharmacological reduction of ER stress protects against TDP-43 neuronal toxicity in vivo. *Neurobiol. Dis.*, **55**, 64–75.
29. Nakatsuka, M., Nakatsuka, K. and Osawa, Y. (1998) Metabolism-based inactivation of penile nitric oxide synthase activity by guanabenz. *Drug Metab. Dispos.*, **26**, 497–501.
30. Boyce, M., Bryant, K.F., Jousse, C., Long, K., Harding, H.P., Scheuner, D., Kaufman, R.J., Ma, D., Coen, D.M., Ron, D. et al. (2005) A selective inhibitor of eIF2alpha dephosphorylation protects cells from ER stress. *Science*, **307**, 935–939.
31. Ramsay, R.R., Dunford, C. and Gillman, P.K. (2007) Methylene blue and serotonin toxicity: inhibition of monoamine oxidase A (MAO A) confirms a theoretical prediction. *Br. J. Pharmacol.*, **152**, 946–951.
32. Urano, F., Calfon, M., Yoneda, T., Yun, C., Kiraly, M., Clark, S.G. and Ron, D. (2002) A survival pathway for *Caenorhabditis elegans* with a blocked unfolded protein response. *J. Cell Biol.*, **158**, 639–646.
33. Madabattula, S.T., Strautman, J.C., Bysice, A.M., O'Sullivan, J. A., Androschuk, A., Rosenfelt, C., Doucet, K., Rouleau, G. and Bolduc, F. (2015) Quantitative analysis of climbing defects in a *Drosophila* model of neurodegenerative disorders. *J. Vis. Exp.*, doi:10.3791/52741.
34. Therrien, M., Rouleau, G.A., Dion, P.A. and Parker, J.A. (2013) Deletion of C9ORF72 results in motor neuron degeneration and stress sensitivity in *C. elegans*. *PLoS One*, **8**, e83450.
35. Tauffenberger, A., Julien, C. and Parker, J.A. (2013) Evaluation of longevity enhancing compounds against transactive response DNA-binding protein-43 neuronal toxicity. *Neurobiol. Aging*, **34**, 2175–2182.
36. Tauffenberger, A. and Parker, J.A. (2014) Heritable transmission of stress resistance by high dietary glucose in *Caenorhabditis elegans*. *PLoS Genet.*, **10**, e1004346.
37. Bolduc, F.V., Bell, K., Cox, H., Broadie, K.S. and Tully, T. (2008) Excess protein synthesis in *Drosophila fragile X* mutants impairs long-term memory. *Nat. Neurosci.*, **11**, 1143–1145.